Design of an OFDM-based Differential Cyclic-Shifted DCSK System for Underwater Acoustic Communications

Xiangming Cai, Luyao Hu, Weikai Xu, Lin Wang
Dept. of Information and Communication Engineering, Xiamen University, Fujian 361005, China
Email:xweikai@xmu.edu.cn

2021 26th IEEE Asia-Pacific Conference on Communications (APCC) | 978-1-7281-7254-5/21/$31.00 ©2021 IEEE | DOI: 10.1109/APCC49754.2021.9609854

***Abstract*—Given the high transmission loss, severe Doppler spread and large multipath delay in the underwater acoustic (UWA) channel, the channel estimation and tracking in the conventional orthogonal frequency division multiplexing (OFDM) based UWA systems are severely unaffordable. In this paper, we propose a low-complexity and cost-friendly OFDM-based differential cyclic-shifted differential chaos shift keying (OFDM-DCS-DCSK) system which offers a high data rate, superior robustness and enhanced system security for UWA communications without the need for channel state information (CSI). In the system, the information bits are carried by different step lengths of the cyclic shifts. At the receiver, a low-complexity detection method is used to search the position of maximum from the cyclic correlation values and therefore estimate the information bits. Finally, simulation results demonstrate the proposed OFDM-DCS-DCSK system outperforms its competitors both in bit error rate (BER) performance and in system security.**

***Index Terms*—Underwater acoustic (UWA) communications, differential chaos shift keying (DCSK), cyclic shift, orthogonal frequency division multiplexing (OFDM), Fast Fourier Transform.**

I. Introduction

The sea covers more than 70% of the earth's surface, however, up to 95% of the ocean still remains a mystery, which has not been explored and developed sufficiently so far [1], [2]. It is clear underwater information transmission is capable of benefiting pollution monitoring, offshore resource exploration and other economic gains. Therefore, information transmission in the marine environment has drawn increasing attention in industrial and scientific community. One of the most crucial demands on establishing the marine communication networks and internet of underwater things (IoUT) [3] is to enable various underwater devices to be interconnected closely for data transmission and information sharing in a low-cost manner.

Underwater acoustic (UWA) communications are a rapidly growing field of engineering and science research, driven by the expansion of applications which require underwater data transmission without wired connections [4]. The orthogonal frequency division multiplexing (OFDM) technique, which divides the frequency-selective wideband channel into overlapping but orthogonal multi-carrier narrowband subchannels, is an effective solution to address the large multpath delay and even the time-varying distortion in terrestrial wireless communications as well as in UWA communications [5]. An adaptive-modulated OFDM system was presented in [6] for time-varying UWA links with at-sea experiments. It is shown the adaptive-modulated scheme provides significant throughput improvements compared to the non-adaptive one at the same target bit error rate (BER) level.

However, the conventional OFDM-based UWA systems heavily depend on the channel state information (CSI) acquired via channel estimation [7]–[9]. For the underwater channel, the long propagation delay and time-varying properties make the channel estimation almost unaffordable. More importantly, the CSI collected at the receiver may not reflect the actual UWA channel especially when the transmitted signal travels a long way [10]. Although the error-correcting codes such as low-density parity-check codes (LDPC) [11], [12] potentially have good performance in the fading channel, the time-varying property of the UWA channel degrades the BER performance significantly [13]. In this perspective, ultra-robust and cost-effective signal designs are all-important directions in physical layer for UWA communications.

Chaotic signals can be generated by simple electronic circuits [14] and they have many superior properties, including noise-like, wideband, sensitivity to initial conditions and unpredictability for a long time [15]. These properties make chaotic signals naturally suitable for spread-spectrum (SS) communications. The key idea for the exploitation of chaotic signals in SS communications is to increase the robustness against the multipath propagation [16], [17]. The benefit of spreading the signal power over a wide frequency range in a chaotic manner is to transmit the information-bearing signal below the average noise floor, decreasing the risk of being eavesdropped by an illegal receiver.

A robust non-coherent differential chaos shift keying (DCSK) [18], exploiting the transmitted-reference (TR) approach, is capable of eliminating the need for complex chaos synchronization by invoking the simple correlation operation. Specifically, DCSK schemes can not only mitigate the adverse effects of multipath fading without requiring CSI, but also show high resistance against the multipath delay [19]. Consequently, the DCSK scheme is a low-complexity solution for different applications in Internet of things (IoTs), especially non-stationary scenarios. There has been many proposals applying DCSK-based schemes to various scenarios, including UWA communications [20], power line communications [21], coded modulation systems [22], tactile Internet [23] and e-health IoT applications [24]. However, DCSK

978-1-7281-7254-5/21/$31.00 ©2021 IEEE

is limited by low data rate and poor security. In addition, if channel coefficients vary faster than the bit duration, the BER performance of DCSK would be degraded [25].

To increase the data rate, a multilevel code-shifted M-ary DCSK scheme was proposed in [26] where the M-ary constellation symbols are transmitted by different Walsh codes. Subsequently, the indices of the spreading codes in code-shifted schemes are fully exploited in [27]–[29] to transmit additional information bits in an implicit manner with the aid of code index modulation. The authors of [30] applied the code shift technique in a DCSK system and proposed an OFDM-based code-shifted DCSK (OFDM-CS-DCSK) scheme to combat the severe frequency-selective fading channel. However, the number of subcarriers depends on the spreading factor, which limits the applications of OFDM-CS-DCSK. To tackle this problem, a parallel OFDM-based CS-DCSK (P-OFDM-CS-DCSK) system proposed in [20] allows flexible configurations for subcarriers, where multiple CS-DCSK symbols are loaded into the OFDM modulator in a parallel manner.

However, the sophisticated and challenging UWA channel still poses a threat on the code-shifted DCSK schemes because such a code-shifted configuration is quite sensitive to the large multipath delay [27]. The synchronization for Walsh codes is also an intractable issue in the time-varying UWA channel. In addition, synchronization errors results from the long transmission links also penalize the BER performance significantly. Although the continuous-mobility DCSK (CM-DCSK) [25] can partially handle the motion-induced Doppler distortion and spread, its data rate and system security is not satisfactory. The CM-DCSK system only conveys one bit in each transmission duration. Moreover, each reference sample is followed by its corresponding information-bearing sample and this structure makes the transmitted bit detectable by a simple correlation operation.

Motivated by what has been discussed so far, a low-complexity and cost-friendly OFDM-based differential cyclic-shifted differential chaos shift keying (OFDM-DCS-DCSK) system is proposed in this paper (i) to avoid the prohibitively expensive overheads spent on channel estimation in conventional OFDM-based UWA schemes, (ii) to enhance the system security by shifting the chaotic sequence in a cyclic manner and (iii) to obtain a better BER performance compared to the P-OFDM-CS-DCSK system.

The remainder of this paper is organized as follows: Section II details the system model of OFDM-DCS-DCSK as well as the UWA channel. Section III presents the simulation results. Finally, Section IV concludes the paper.

II. The OFDM-DCS-DCSK System

A. The Transmitter

Fig. 1 shows the block diagram of the OFDM-DCS-DCSK transmitter. The total number of transmitted bits is $(M-1)n$ which is partitioned into $M-1$ groups and each group contains n bits. If the transmitted bits are expressed in a vector form, it gives $\mathbf{B} = [\mathbf{b}_1, \mathbf{b}_2, \cdots, \mathbf{b}_{M-1}]$, where $\mathbf{b}_m = [b_{m,1}, b_{m,2}, \cdots, b_{m,n}]$

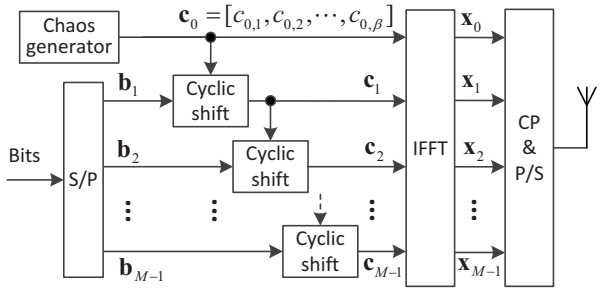

Fig. 1. Block diagram of the OFDM-DCS-DCSK transmitter.

denotes the transmitted bits in the m-th group. Then, the n information bits $\{b_{m,1}, b_{m,2}, \cdots, b_{m,n}\}$ are converted into a decimal number, denoted by ω_m. Particularly, ω_m can be also referred to as the step length of the cyclic shift. Note that the proposed OFDM-DCS-DCSK system uses cyclic shifts of a chaotic signal to convey the information bits, with each shift representing n bits of information.

At the transmitter, a length-β chaotic sequence, $\mathbf{c}_0 = [c_{0,1}, c_{0,2}, \cdots, c_{0,\beta}]$, is produced by a chaos generator, where $\beta = 2^n$ is defined as the spreading factor. The resultant chaotic sequence is placed in the first subcarrier as the reference signal. The $(m-1)$-th chaotic signal, $\mathbf{c}_{m-1}$, is loaded into a cyclic shift block to get the m-th cyclic-shifted chaotic signal $\mathbf{c}_m$, yielding

$$\mathbf{c}_m = \begin{cases} \mathbf{c}_0, & m = 0 \\ \text{circshift}\left(\mathbf{c}_{m-1}, \omega_m\right), & m = 1, 2, \cdots, M-1 \end{cases} \tag{1}$$

where $\text{circshift}(\mathbf{a}, \Delta)$ denotes the cyclic shift operation, which circularly shifts the values in the vector $\mathbf{a}$ by Δ elements. If Δ is 0, the values in vector $\mathbf{a}$ are not shifted.

After processing by the inverse fast Fourier transform (IFFT) module, the i-th subcarrier in the k-th OFDM symbol is expressed as

$$x_{i,k} = \frac{1}{\sqrt{M}} \sum_{m=0}^{M-1} c_{m,k} e^{j\frac{2\pi m i}{M}} \tag{2}$$

where $i = 0, 1, \cdots, M-1$ and $k = 1, 2, \cdots, \beta$. In addition, $c_{m,k}$ is the k-th chaotic chip transmitted in the m-th subcarrier. After β IFFT operations, the resultant signal is formulated as

$$\begin{aligned} \mathbf{X} &= \left[\mathbf{x}_0^{\mathrm{T}}, \mathbf{x}_1^{\mathrm{T}}, \cdots, \mathbf{x}_{M-1}^{\mathrm{T}}\right]^{\mathrm{T}} \\ &= \begin{bmatrix} x_{0,1} & x_{0,2} & \cdots & x_{0,\beta} \\ x_{1,1} & x_{1,2} & \cdots & x_{1,\beta} \\ \vdots & \vdots & \ddots & \vdots \\ x_{M-1,1} & x_{M-1,2} & \cdots & x_{M-1,\beta} \end{bmatrix} \end{aligned} \tag{3}$$

where each column of $\mathbf{X}$ is an OFDM symbol and there are β OFDM symbols transmitted in an OFDM-DCS-DCSK symbol duration. Then, the series-to-parallel conversion is performed on $\mathbf{X}^{\mathrm{T}}$, yielding

$$\begin{aligned} \mathbf{X}_R &= \text{reshape}\left(\mathbf{X}^{\mathrm{T}}, 1, M\beta\right) \\ &= [x_{0,1}, \cdots, x_{0,\beta}, \cdots, x_{M-1,1}, \cdots, x_{M-1,\beta}] \end{aligned} \tag{4}$$

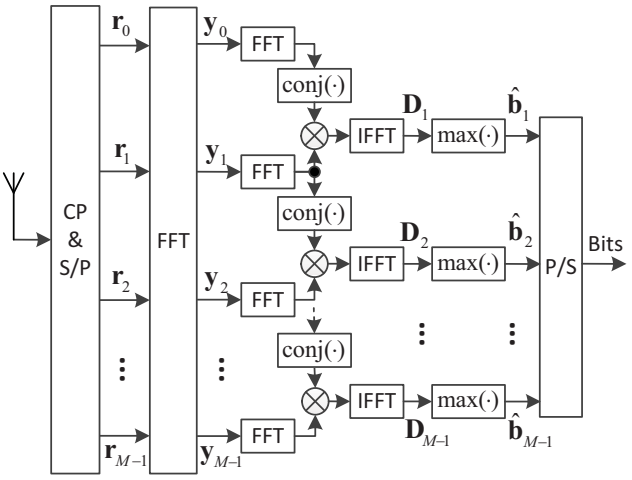

Fig. 2. Block diagram of the OFDM-DCS-DCSK receiver.

where $\mathbf{G} = \mathrm{reshape}(\mathbf{A}, m, n)$ returns the m-by-n matrix $\mathbf{G}$ whose elements are taken column-wise from $\mathbf{A}$. After inserting the cyclic prefix (CP) into the head of $\mathbf{X}_R$, the resultant signal is transmitted in the channel.

B. The UWA Channel

The UWA channel is wideband in nature and characterized by large Doppler shifts and time-varying multipath delays. A widely studied UWA channel developed in [31], which takes the effects of inevitable random local displacements, frequency-dependent attenuation and bottom/surface reflections into account, is used in this paper. The time-varying channel response of the UWA channel is modeled as

$$\tilde{H}(f,t) = \bar{H}_0(f) \sum_{p=1}^{L} \lambda_p \tilde{\gamma}_p(f,t) e^{-j2\pi f \tau_p} \tag{5}$$

where $\bar{H}_0(f)$ gives the filtering effect for all the paths between the transmitter and receiver, L is the number of paths and λ_p is the channel coefficient of the p-th path which travels the channel with a delay of τ_p. In addition, the overall small-scale path coefficient is defined as

$$\tilde{\gamma}_p(f,t) = \gamma_p(f,t) e^{j2\pi a_p f t} \tag{6}$$

which is used to describe displacements on the order of one or a few wavelengths. $a_p = v_p/c$ denotes the Doppler factor corresponding to the velocity v_p, and specifically the Doppler shift is a composite effect of the surface wave perturbations, relative source-receiver drifts and vehicular motion. When the IFFT operation is performed on the channel transfer function $\tilde{H}(f,t)$, it gives the pulse response of the UWA channel, expressed as $h(\tau,t) = \mathcal{F}^{-1}\{\tilde{H}(f,t)\}$, where $\mathcal{F}^{-1}\{\cdot\}$ denotes the IFFT operator.

C. The Receiver

The receiver structure of the OFDM-DCS-DCSK system is illustrated in Fig. 2. At the receiver, the CP is first removed from the received signal and the resultant serial signal is converted into several parallel ones. Then, these parallel signals are sent into the FFT module. The k-th chaotic chip in the m-th subcarrier is obtained as

$$y_{m,k} = \frac{1}{\sqrt{M}} \sum_{i=0}^{M-1} r_{i,k} e^{-j\frac{2\pi m i}{M}} \tag{7}$$

for $m = 0, 1, \cdots, M-1$. After performing the FFT operations β times, the resultant signal is collected to form

$$\begin{aligned} \mathbf{Y} &= \left[\mathbf{y}_0^{\mathrm{T}}, \mathbf{y}_1^{\mathrm{T}}, \cdots, \mathbf{y}_{M-1}^{\mathrm{T}}\right]^{\mathrm{T}} \\ &= \begin{bmatrix} y_{0,1} & y_{0,2} & \cdots & y_{0,\beta} \\ y_{1,1} & y_{1,2} & \cdots & y_{1,\beta} \\ \vdots & \vdots & \ddots & \vdots \\ y_{M-1,1} & y_{M-1,2} & \cdots & y_{M-1,\beta} \end{bmatrix}. \end{aligned} \tag{8}$$

In order to retrieve the information bits, the OFDM-DCS-DCSK receiver needs to detect a maximum absolute value from the elements of the periodic correlation vector. If the receiver performs a brute-force correlation, the computational complexity is severally unaffordable, especially when β is large. Considering the low-cost demand of UIoT applications, we perform a simple search algorithm, expressed as

$$\mathbf{D}_u = \mathcal{F}^{-1}\left\{\mathrm{conj}\left[\mathcal{F}\left(\mathbf{y}_{u-1}\right)\right] \times \mathcal{F}\left(\mathbf{y}_u\right)\right\} \tag{9}$$

for $u = 1, 2, \cdots, M-1$. Notation $\mathrm{conj}(\cdot)$ denotes the conjugate operator while $\mathcal{F}(\cdot)$ is the FFT operator. Furthermore, $\times$ is a term-by-term multiplication. $\mathbf{y}_u = [y_{u,1}, y_{u,2}, \cdots, y_{u,\beta}]$ is the signal transmitted by the u-th subcarrier. The elements of the vector $\mathbf{D}_u$ by using (9) are $\{D_{u,1}, D_{u,2}, \cdots, D_{u,\beta}\}$. Therefore, the estimated step length of the cyclic shift can be obtained by finding the maximum value from set $\{|D_{u,k}|\}_{k=1}^{\beta}$, formulated as

$$\hat{\omega}_u = \underset{k \in \{1,2,\cdots,\beta\}}{\arg\max} \{|D_{u,k}|\} \tag{10}$$

where $|D_{u,k}|$ is to get the absolute value of $D_{u,k}$. After converting the estimated step length $\hat{\omega}_u$ into n binary numbers, the corresponding transmitted bits $\hat{\mathbf{b}}_u$ are finally recovered.

III. Simulation Results and Discussion

In this section, the system security and BER performance of OFDM-DCS-DCSK are evaluated and compared to its competitors. At first, the square of signal waveform for the OFDM-DCS-DCSK and P-OFDM-CS-DCSK [20] systems are shown in Fig. 3. In simulations, $M = 16$ and $\beta = 64$ are used in both systems. Furthermore, the order of Walsh code $W_o = 4$ is applied in P-OFDM-CS-DCSK. Although the reference and information-bearing signals are overlapped in the same time slots in P-OFDM-CS-DCSK, the similarity between different subcarriers is not fully eradicated. For example, as observed at the top of Fig. 3, the waveform in the solid box is same as that in the dash box. More importantly, the waveforms in each box also display periodic behavior which jeopardizing the security of P-OFDM-CS-DCSK. In contrast, the waveform at the bottom of Fig. 3 is almost irregular which indicates the OFDM-DCS-DCSK system has higher security.

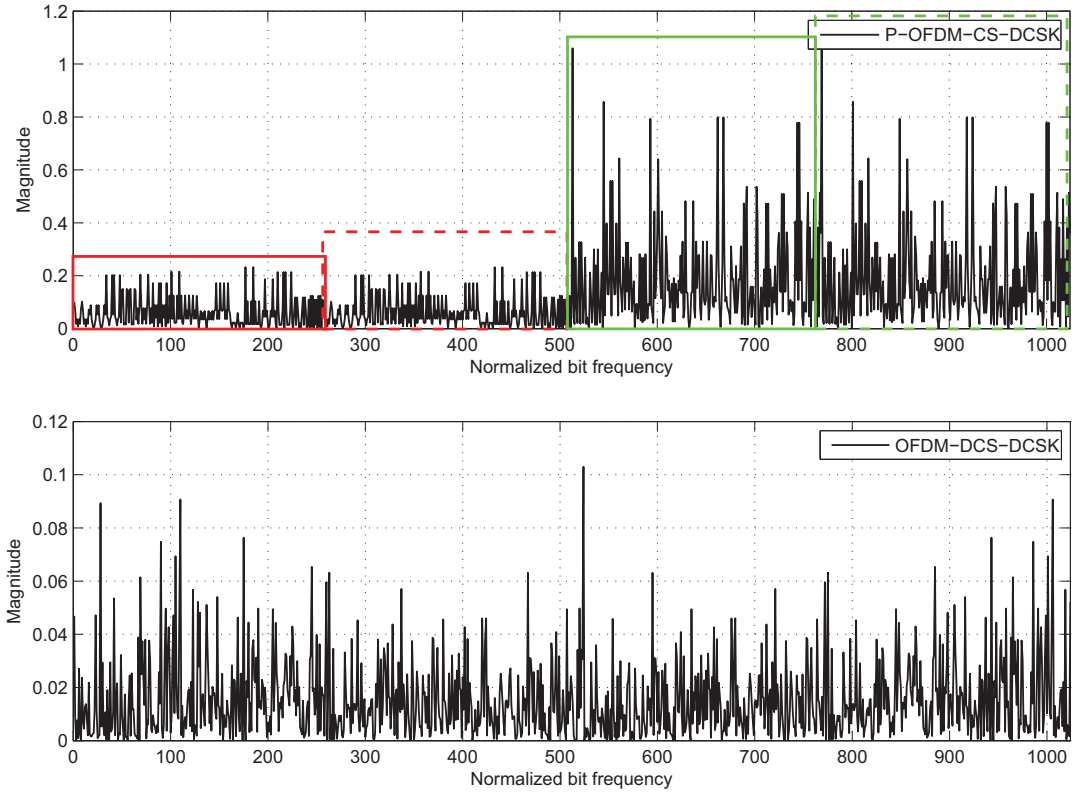

Fig. 3. Magnitude of frequency components versus normalized bit frequency for the square of the signal sample.

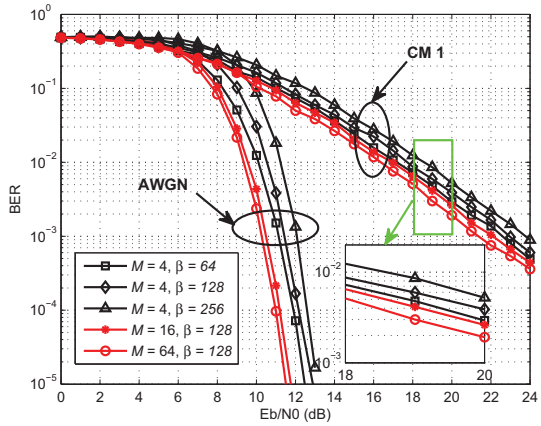

Fig. 4. The effects of M and β on the BER performance of OFDM-DCS-DCSK over AWGN and CM 1 channels.

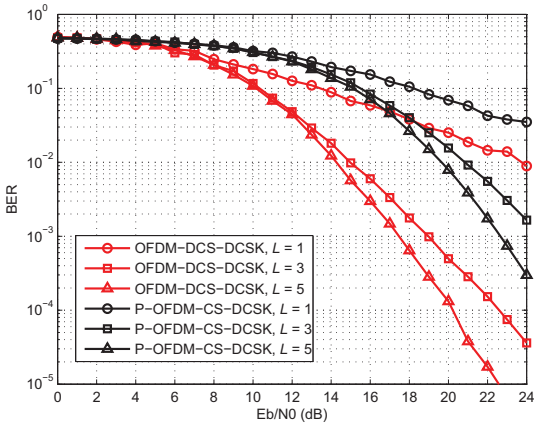

Fig. 5. BER performance comparison between OFDM-DCS-DCSK and P-OFDM-CS-DCSK over the CM 2 channel with different L.

Next, the effects of β and M on the BER performance of OFDM-DCS-DCSK are studied in Fig. 4. Here, a general additive white Gaussian noise (AWGN) and a Doppler-spreading-free Rayleigh fading channel (referred to as CM 1 channel), with channel coefficients $E[\lambda_p] = e^{-0.1(p-1)}, p = 1, 2$ and path delays $\{0, 2\}$, are used in the simulations of Fig. 4. The length of cyclic prefix, denoted by ϱ, is set to 4. It is shown that the OFDM-DCS-DCSK system degrades the BER performance with an increased β. Furthermore, when M is increased from 4 to 64, OFDM-DCS-DCSK performs better and its improvement in BER performance is more than 1dB at BER=10^{-5} in the AWGN channel. The main reason is the ratio of energy spent on the information-bearing signals to that on the reference signal is increased with a large M, which contributes to the improvement in BER performance.

In Fig. 5, the BER performance of the OFDM-DCS-DCSK

TABLE I
UWA CHANNEL PARAMETERS

Channel type	UWA-I	UWA-II
Ocean depth (m)	100	50
Transmitter depth (m)	90	20
Receiver depth (m)	50	10
Channel distance (m)	1000	500
Spreading coefficient	1.7	1.7
Range of frequency (kHz)	[10,20]	[10,20]
Sound speed in water, c_w (m/s)	1500	1500
Sound speed in bottom, c_b (m/s)	1200	1200
Surface variance, σ_s^2	1.125	1.125
Bottom variance, σ_b^2	0.5	0.5
$B_{\delta,p}(Hz)^{\dagger}$	0.05	0.05
Number of intra-paths, S_p	20	20
Mean of intra-path amplitudes, μ_p	0.3	0.3
Variance of intra-path amplitudes, υ_p	10^{-4}	10^{-4}
Surface variation amplitude, A_w (m)	0.05	0.7
Surface variation frequency, f_w (Hz)	0.01	0.01

† $B_{\delta,p}$ is 3dB width of the power spectrum density of intra-path delays.

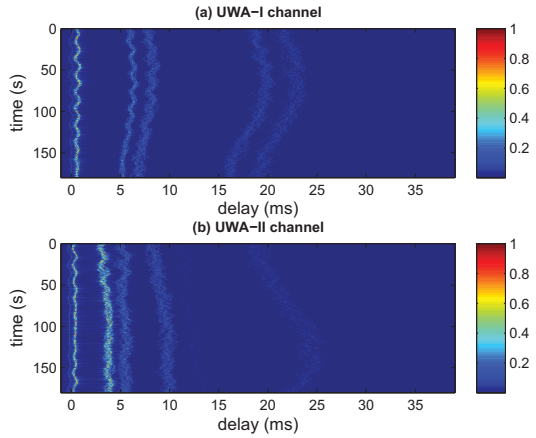

Fig. 6. Acoustic channel impulse response based on the model developed in [31].

system is compared to that of P-OFDM-CS-DCSK over the fading channel with different number of paths L. A common multipath Rayleigh fading channel with the same channel coefficients, which is referred to as CM 2, is used in simulations. $\varrho = 10$ is used in the simulations. Furthermore, the spreading factor and the number of subcarriers are set to 128 and 16, respectively. $W_o = 4$ is used in P-OFDM-CS-DCSK's simulations. As shown in Fig. 5, both OFDM-DCS-DCSK and P-OFDM-CS-DCSK can harvest a good diversity gain when L is increased from 1 to 5. It is worth noting that the proposed OFDM-DCS-DCSK system is capable of offering more than 5dB gain in BER performance compared to P-OFDM-CS-DCSK at the BER of 10^{-3}.

Finally, we evaluate the BER performance of OFDM-DCS-DCSK in two different UWA channels and compare to P-OFDM-CS-DCSK. The main simulation parameters for the UWA channels are tabulated in Table I. Moreover, the corresponding time-

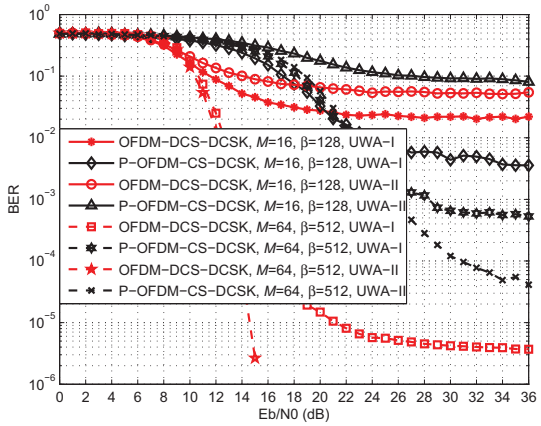

Fig. 7. BER performances of OFDM-DCS-DCSK and P-OFDM-CS-DCSK in different UWA channels.

varying channel impulse responses for UWA-I and UWA-II channels are depicted in Fig. 6. Here, $\varrho = 10$ is used in the simulations of both systems. As observed in Fig. 7, the OFDM-DCS-DCSK system with $M = 16$ and $\beta = 128$ reaches to the error floor quickly in both UWA-I and UWA-II channels. However, when $M = 64$ and $\beta = 512$, the error floor is decreased because a larger spreading length allows OFDM-DCS-DCSK to combat inter-symbol interference caused by the UWA channels. In addition, for a large β, the OFDM-DCS-DCSK system offers a better BER performance than P-OFDM-CS-DCSK in two different UWA channels.

IV. CONCLUSION

In this paper, a low-complexity OFDM-based cyclic-shifted differential chaos shift keying has been proposed, where the cyclic-shifted steps of the information-bearing subcarriers are used to transmit the information bits. Since the chaotic chips in the adjacent subcarriers are absolutely different, the system security of OFDM-DCS-DCSK is enhanced to a large extent. In addition, compared to the P-OFDM-CS-DCSK and conventional coherent OFDM systems, the proposed OFDM-DCS-DCSK system does not need the Walsh code synchronization and channel estimation at its receiver, which meets the low-complexity requirements of UIoT devices. After evaluating the security and BER performance of OFDM-DCS-DCSK, it concludes that (i) OFDM-DCS-DCSK has higher security than P-OFDM-CS-DCSK due to the cyclic-shifted chaotic structure of different subcarriers; (ii) OFDM-DCS-DCSK offers better BER performance in contrast to P-OFDM-CS-DCSK.

ACKNOWLEDGEMENT

This work was supported in part by the Natural Science Foundation (NSF) of China under Grant No. 61871337 and 61671395.

REFERENCES

[1] Y. Li, S. Wang, C. Jin, Y. Zhang and T. Jiang, "A survey of underwater magnetic induction communications: Fundamental issues, recent advances, and challenges," *IEEE Commun. Survey Tut.*, vol. 21, no. 3, pp. 2466-2487, thirdquarter 2019.

[2] S. N. Oishimaya, *How Much of the Ocean Is Still Unexplored*, 2018. [Online]. Available: https://www.worldatlas.com/articles/how-much-of-the-ocean-is-still-unexplored.html

[3] M. C. Domingo, "An overview of the Internet of underwater things," *J. Netw. Comput. Appl.*, vol. 35, no. 6, pp. 1879-1890, Nov. 2012.

[4] M. Stojanovic, "High-speed underwater acoustic communications," in *Underwater Acoustic Digital Signal Processing and Communication Systems*. New York, NY, USA: Springer, 2002, pp. 1-35.

[5] M. T. Altabbaa, "Double Focusing: A new sparse channel estimation algorithm for doubly selective SFBC-OFDM-based underwater acoustic systems," *IEEE Wireless Commun. Lett.*, vol. 9, no. 12, pp. 2040-2044, Dec. 2020.

[6] A. Radosevic, R. Ahmed, T. M. Duman, J. G. Proakis, and M. Stojanovic, "Adaptive OFDM modulation for underwater acoustic communications: Design considerations and experimental results," *IEEE J. Ocean. Eng.*, vol. 39, no. 2, pp. 357-370, Apr. 2014.

[7] T. Kang and R. A. Iltis, "Iterative carrier frequency offset and channel estimation for underwater acoustic OFDM systems," *IEEE J. Sel. Areas Commun.*, vol. 26, no. 9, pp. 1650-1661, December 2008.

[8] C. R. Berger, S. Zhou, J. C. Preisig, and P. Willett, "Sparse channel estimation for multicarrier underwater acoustic communication: From subspace methods to compressed sensing," *IEEE Trans. Signal Process.*, vol. 58, no. 3, pp. 1708-1721, Mar. 2010.

[9] Z. Wang, Y. Li, C. Wang, D. Ouyang and Y. Huang, "A-OMP: An adaptive OMP algorithm for underwater acoustic OFDM channel estimation," *IEEE Wireless Commun. Lett.*, doi: 10.1109/LWC.2021.3079225.

[10] M. Stojanovic and J. Preisig, "Underwater acoustic communication channels: Propagation models and statistical characterization," *IEEE Commun. Mag.*, vol. 47,no. 1, Jan. 2009, pp. 84-89.

[11] Y. Fang, P. Chen, G. Cai, F. C. M. Lau, S. C. Liew, and G. Han, "Outage-limit-approaching channel coding for future wireless communications: Root-protograph low-density parity-check codes," *IEEE Veh. Technol. Mag.*, vol. 13, no. 2, pp. 85-93, 2019.

[12] Y. Fang, S. Liew, and T. Wang, "Design of distributed protograph LDPC codes for multi-relay coded-cooperative networks," *IEEE Trans. Wireless Commun.*, vol. 16, no. 11, pp. 7235-7251, Nov. 2017.

[13] J. Huang, S. Zhou and P. Willett, "Nonbinary LDPC coding for multicarrier underwater acoustic communication," *IEEE J. Sel. Areas Commun.*, vol. 26, no. 9, pp. 1684-1696, Dec. 2008.

[14] M. Eisencraft, R. Attux, and R. Suyama, *Chaotic Signals in Digital Communications*. Boca Raton, FL, USA: CRC Press, 2013.

[15] Y. Fang, G. Han, P. Chen, F. C. M. Lau, G. Chen and L. Wang, "A survey on DCSK-based communication systems and their application to UWB scenarios," *IEEE Commun. Survey Tut.*, vol. 18, no. 3, pp. 1804-1837, third quarter 2016.

[16] F. C. M. Lau and C. K. Tse, *Chaos-Based Digital Communication Systems*. New York, NY, USA: Springer, 2003.

[17] A. Abel and W. Schwarz, "Chaos communications-principles, schemes, and system analysis," *Proc. IEEE*, vol. 90, no. 5, pp. 691-710, May 2002.

[18] G. Kolumbán, G. K. Vizvari, W. Schwarz, and A. Abel, "Differential chaos shift keying: A robust coding for chaos communication," in *Proc. Nonlinear Dyn. Electron. Syst.*, Seville, Spain, 1996, pp. 92-97.

[19] Y. Xia, C. K. Tse, and F. C. M. Lau, "Performance of differential chaos-shift-keying digital communication systems over a multipath fading channel with delay spread," *IEEE Trans. Circuits Syst., II, Exp. Briefs*, vol. 51, no. 12, pp. 680-684, Dec. 2004.

[20] M. Chen, W. Xu, D. Wang and L. Wang, "Multi-carrier chaotic communication scheme for underwater acoustic communications," *IET Commun.*, vol. 13, no. 14, pp. 2097-2105, 27 8 2019.

[21] G. Kaddoum and N. Tadayon, "Differential chaos shift keying: A robust modulation scheme for power-line communications," *IEEE Trans. Circuits Syst., II, Exp. Briefs*, vol. 64, no. 1, pp. 31-35, Jan. 2017.

[22] P. Chen, L. Shi, G. Cai, L.Wang, and G. Chen, "A coded DCSK modulation system over Rayleigh fading channels," *IEEE Trans. Commun.*, vol. 66, no. 9, pp. 3930-3942, Sept. 2018.

[23] H. Ma, G. Cai, Y. Fang, J. Wen, P. Chen and S. Akhtar, "A new enhanced energy-detector-based FM-DCSK UWB system for tactile Internet," *IEEE Trans. Ind. Inform.*, vol. 15, no. 5, pp. 3028-3039, May 2019.

[24] G. Cai, Y. Fang, P. Chen, G. Han, G. Cai and Y. Song, "Design of an MISO-SWIPT-aided code-index modulated multi-carrier M-DCSK system for e-health IoT," *IEEE J. Sel. Areas Commun.*, vol. 39, no. 2, pp. 311-324, Feb. 2021.

[25] F. J. Escribano, G. Kaddoum, A. Wagemakers and P. Giard, "Design of a new differential chaos-shift-keying system for continuous mobility," *IEEE Trans. Commun.*, vol. 64, no. 5, pp. 2066-2078, May 2016.

[26] X. Cai, W. Xu, R. Zhang and L. Wang, "A multilevel code shifted differential chaos shift keying system with M-ary modulation," *IEEE Trans. Circuits Syst. II, Exp. Briefs.*, vol. 66, no. 8, pp. 1451-1455, Aug. 2019.

[27] X. Cai, W. Xu, D. Wang, S. Hong and L. Wang, "An M-ary orthogonal multilevel differential chaos shift keying system with code index modulation," *IEEE Trans. Commun.*, vol. 67, no. 7, pp. 4835-4847, Jul. 2019.

[28] G. Cai, Y. Fang, J. Wen, S. Mumtaz, Y. Song and V. Frascolla, "Multi-carrier M-ary DCSK system with code index modulation: An efficient solution for chaotic communications," *IEEE J. Sel. Topics Signal Process.*, vol. 13, no. 6, pp. 1375-1386, Oct. 2019.

[29] X. Cai, W. Xu, S. Hong and L. Wang, "A trinal-code shifted differential chaos shift keying system," *IEEE Commun. Lett.*, vol. 25, no. 3, pp. 1000-1004, Mar. 2021.

[30] M. Chen, W. Xu, D. Wang, and L. Wang, "Design of a multi-carrier different chaos shift keying communication system in doubly selective fading channels," in *Proc. 23rd Asia-Pac. Conf. Commun. (APCC)*, Dec. 2017, pp. 1-6.

[31] P. Qarabaqi and M. Stojanovic, "Statistical characterization and computationally efficient modeling of a class of underwater acoustic communication channels," *IEEE J. Ocean. Eng.*, vol. 38, no. 4, pp. 701-717, Oct. 2013.